J Comput Aided Mol Des (2008) 22:799–814
DOI 10.1007/s10822-008-9215-6

Molecular dynamics simulations of ligand-induced backbone conformational changes in the binding site of the periplasmic lysine-, arginine-, ornithine-binding protein

Ami Y.-C. Yang · Ricardo L. Mancera

Received: 10 December 2007 / Accepted: 1 April 2008 / Published online: 15 April 2008

Abstract The periplasmic lysine-, arginine-, ornithine-binding protein (LAOBP) traps its ligands by a large hinge bending movement between two globular domains. The overall geometry of the binding site remains largely unchanged between the open (unliganded) and closed (liganded) forms, with only a small number of residues exhibiting limited movement of their side chains. However, in the case of the ornithine-bound structure, the backbone peptide bond between Asp11 and Thr12 undergoes a large rotation. Molecular dynamics simulations have been used to investigate the origin and mechanism of this backbone movement. Simulations allowing flexibility of a limited region and of the whole binding site, with and without bound ligands, suggest that this conformational change is induced by the binding of ornithine, leading to the stabilisation of an energetically favourable alternative conformation.

Keywords LAO binding protein · Molecular dynamics · Protein flexibility

Introduction

One of the main difficulties facing the use of molecular modelling methods in the drug discovery process is the representation of the intrinsic molecular flexibility of the protein receptor and the conformational changes that take place upon ligand binding [1–6]. The simplest approaches model side chain flexibility by means of either rotamer libraries of likely side chain conformations [1–7] or through the optimisation of side chain torsional angles [8–12]. Other approaches involve the use of an ensemble of protein structures derived from molecular dynamics simulations [13, 14] or multiple crystal structures or NMR ensembles [15–21]. So called 'soft docking' methods allow for overlap of protein and ligand after relaxing the penalty for steric clash [22–24]. Hybrid approaches combine multiple experimentally determined protein structures with a pharmacophore representation of the binding site [25–27]. Protein flexibility in ligand-protein docking has also been modelled by running explicit solvent molecular dynamics simulations [28–31].

Comparisons of unbound and ligand-bound proteins have suggested that relatively few amino acid side chains undergo conformational changes upon ligand binding [31]. Previous studies have shown that for most proteins with limited backbone motion, the use of rotamer libraries is sufficient to predict low energy conformations of their binding sites [32]. However, there is also evidence that considering only side chain flexibility may result in the neglect of significant main chain conformational changes, which in turn can influence side chain conformations [33].

The use of a rotamer library to predict an alternative conformation of the binding site of the lysine-, arginine-, ornithine-binding protein (LAOBP) failed to reproduce a critical conformational change of a single sidechain due to the neglect of a simultaneous backbone peptide bond rotation [32]. The rest of the protein backbone was determined to exhibit very little movement across all ligand-bound crystal structures [32]. Consequently this protein

A. Y.-C. Yang
Department of Pharmacology, University of Cambridge, Tennis Court Road, Cambridge CB2 1PD, UK

R. L. Mancera (✉)
Western Australian Biomedical Research Institute, School of Pharmacy and School of Biomedical Sciences, Curtin University of Technology, GPO Box U1987, Perth, WA 6845, Australia
e-mail: R.Mancera@curtin.edu.au

represents an excellent case study of the ability of molecular dynamics simulations to predict alternative conformations of the binding site of a protein after a single backbone peptide bond rotation.

The LAOBP is made up of two globular domains, each one consisting of five β-strands and four α-helices, with both domains held together by two short connecting peptide segments [34]. The substrate binding site is located in a deep cleft between the two domains [35], as shown in Fig. 1a. The LAOBP transports basic amino acids by capturing them through a large relative hinge movement between its two domains and sequestering the ligands in the buried cleft [36]. These domains are far apart in the unliganded 'open' form but come into contact with each other in the ligand-bound 'closed' form after a large-scale hinge movement [35, 37]. This mechanism of substrate binding is common in the binding protein family, and the two conformations produced by this type of hinge domain movement are likely to be distinguished by a membrane-bound transport complex as part of the process of release and translocation of the ligand into the cell cytoplasm [36, 38]. The LAOBP has high affinity for its ligands, as revealed by the K_d values: arginine (14 nM), lysine (15 nM), ornithine (30 nM) and histidine (500 nM) [39].

The crystal structure of the LAOBP has been determined in its apo-state (unbound) [34] and bound to lysine [35], arginine [37], ornithine [37] and histidine [37]. These structures reveal no direct or indirect (water-mediated) contacts between the ligands and the inter-domain connecting strands, suggesting that these ligands do not induce the conformational change directly but merely stabilise the closed conformation. Bound ligands are buried deep within the protein and have zero solvent accessibility. There are several residues that provide ionic or hydrophilic (Asp11, Ser70, Ser72, Arg77, Thr121 and Asp161), water-mediated (Asp30 and Ser 69) and hydrophobic (Tyr14, Phe52 and Leu117) interactions with the ligands. Most side chains in the binding site have the same conformation in both the open and closed forms, with the exception of Asp11, Tyr14 and Ser72 (additionally Asp171 in the case of bound arginine). All ligands (except arginine) interact with water molecules W401 and, indirectly, W402. These tightly-bound water molecules are also present in the unbound form of the protein (hence their role is to neutralise the charges of the protein atoms). Binding of the larger arginine requires the displacement of W401 into the bulk solvent.

Asp11 is the only residue of the binding site that adopts a different side chain *and* backbone conformation in the ornithine-bound complex. Ornithine is the smallest of all ligands and the empty space that it leaves is not occupied by a water molecule but by the side chain of Asp11, with which it forms a salt bridge. Incidentally, histidine does not appear to be able to establish such ionic interaction with Asp11 and does not induce such conformational change, which might explain its reduced binding affinity. The conformational change of the side chain of Asp11 would be impossible without the concomitant rotation of the peptide bond between Asp11 and Thr12 because of the steric clash between the carbonyl oxygen and the carboxyl group of Asp11. The peptide bond undergoes a large 122° rotation as a consequence of changes in the backbone torsion angle in the two residues: the Φ/ψ angles of Asp11 (−94.5°/112.7°) and Thr12 (−85.0°/32.2°) change to −88.3°/−15.1° and

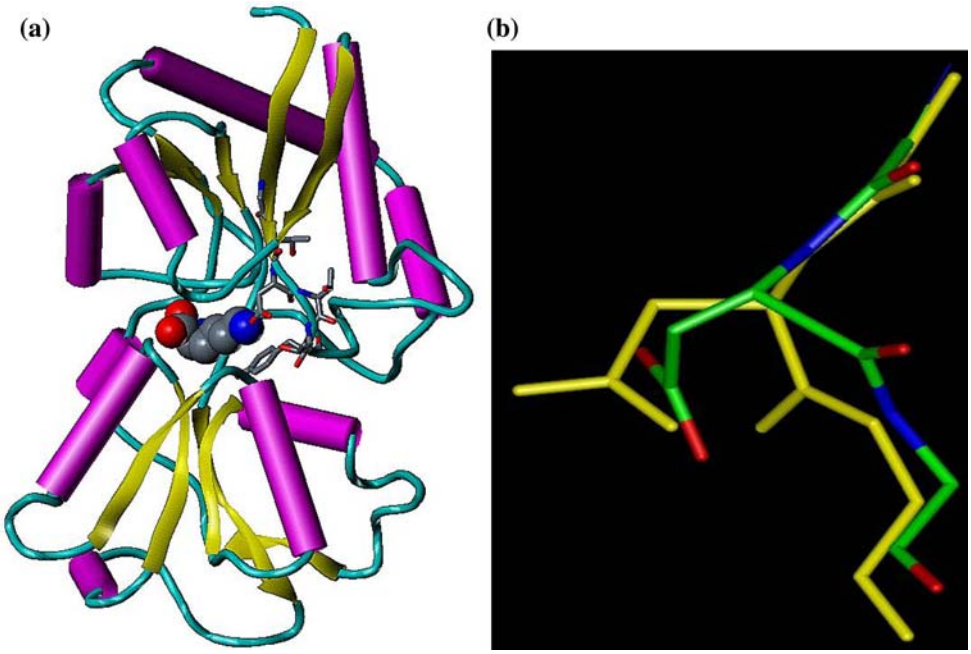

Fig. 1 The lysine-, arginine-, ornithine-binding protein. (**a**) Cartoon representation of the overall structure of the LAOBP in its closed conformation (PDB structure 1LST), showing the location of lysine (CPK representation) in the binding site. The 9–14 segment is shown as sticks. (**b**) The two alternative conformations of Asp11 and Thr12: conformation A (from structure 1LST) is shown in yellow sticks and conformation B (from structure 1LAH) is shown in sticks coloured according to atom type

58.3°/9.8°, respectively, both of which correspond to energetically favourable main chain conformations. As a result of these changes, the main chain carbonyl oxygen of Asp11 becomes exposed to the solvent and the side chain becomes buried. Figure 1b illustrates the two conformations of Asp11. The dynamics of Asp11 are thus an interesting test case for ligand-induced conformational changes as it lacks interactions with other residues in the protein and its main interactions are ionic in nature through its side chain to the ligand.

Whilst to our knowledge no investigation has been made of the dynamics of the peptide bond between Asp11 and Thr12, several theoretical studies have investigated the mechanism of the hinge conformational change of the LAOBP. An analysis of the differences in Cα-torsion angles between the open and closed forms showed that one domain undergoes a large displacement with respect to the other domain, and that the domains behave overall like rigid bodies but exhibit some degree of flexibility [40]. Biased probability Monte Carlo minimisations using internal coordinate mechanics have been used to generate structurally diverse low-energy conformations that resemble the open and closed conformations of this protein [41]. The Gaussian Network Model has been used to predict the most cooperative modes of motion of the LAOBP and highlight those regions with different levels of flexibility in the open (unbound) and closed (lysine-bound) conformations [42]. The hinge region was determined to have a high degree of fluctuation whilst ligand-binding residues exhibited minimal flexibility [42]. Other normal modes calculations have equally predicted the low-frequency collective motions of the LAOBP responsible for its interdomain hinge movement [43]. A principal component analysis of collective motions during molecular dynamics simulations of the LAOBP revealed that the presence of a bound ligand stabilises the protein and modulates its pre-existing pattern of flexibility, as similar motions are observed but with reduced magnitude [44]. Transitions between the closed and open forms were observed to occur rapidly (less than 1.0 ns) [44].

We have performed molecular dynamics simulations of the binding site of the LAOBP. The conformational behaviour of the peptide bond between Asp11 and Thr12 is analysed in detail in order to explain the possible role of bound ornithine in inducing these changes and stabilising an alternative backbone conformation that does not exist in other ligand-bound or unbound forms of the protein.

Materials and methods

Initial structural analysis of the LAOBP

Five crystal structures of the LAOBP from *Salmonella typhimurium* have been determined: the open unliganded form (PDB code 2LAO) [34] and the closed liganded forms with lysine (PDB code 1LST) [35], arginine (PDB code 1LAF) [37], ornithine (PDB code 1LAH) [37], and histidine (PDB code 1LAG) [37]. Table 1 lists these structures.

The four liganded structures of the LAOBP were aligned by least squares fit using the McLachlan algorithm [45], as implemented in the program *Profit* [46]. This was a straightforward task as all X-ray structures have similar conformations. All heavy atoms of the protein structures were used for the superimposition. The backbone conformation of the unliganded form of the LAOBP was also compared with the liganded forms. The arginine-bound structure (PDB code 1LAF) was taken as the reference structure for this comparison.

A number of aminoacid residues have been previously defined to be involved in ligand binding: Asp11, Tyr14, Asp30, Phe52, Ser69, Ser70, Ser72, Arg77, Leu117, Ser120, Thr121 and Asp161 [32]. An enlarged binding site was defined by including all heavy atoms of any residue with at least one atom within 6.0 Å of the bound ligand. As a result, the binding site included not only the above residues but also other residues from both domains of the LAOBP as well as the interdomain linker region.

In order to overlay the open and closed conformations effectively, PDB structure 2LAO was superimposed twice onto PDB structure 1LAF. The first superimposition was done by aligning the first domain (residues 1–88 and 195–238) only. The atomic coordinates of all heavy atoms in the first domain and the linker region of PDB structure 2LAO that were part of the binding site (as defined above) were extracted and translated with respect to PDB structure

Table 1 Crystal structures of the LAOBP

PBD code	Ligand	Resolution (Å)	Backbone conformation[a]	RMSD of active site (Å)[b]
1LAF	Arginine	2.06	A	–
1LAG	Histidine	2.06	A	0.11
1LAH	Ornithine	2.06	B	0.25
1LST	Lysine	1.8	A	0.14
2LAO	–	1.9	A	0.16

[a] Conformation of residues Asp11-Thr12

[b] RMSD values are obtained by superposition with the 1LAF structure

1LAF. The second superimposition aligned the second domain (residues 94–181) of PDB structure 2LAO onto PDB structure 1LAF. The atomic coordinates of all heavy atoms that belong to the binding site of PDB structure 2LAO were extracted and translated with respect to PDB structure 1LAF. The two sets of translated atomic coordinates were then combined. The average RMSD of the binding site between any pair of all five structures was measured and found to be no more than 0.25 Å (see Table 1), confirming that the overall conformation in the binding site is essentially the same for all four liganded and the unliganded structures.

The conformation of the peptide bond between residues Asp11 and Thr12 was named as "A" for that seen in all structures, except the ornithine-bound structure (PDB code 1LAH), which was named "B". PDB structure 1LST was chosen for our simulations of conformation A as it is the crystal structure with the highest resolution. Due to the high degree of structural similarity between the two ligand-bound structures, it was straightforward to perform molecular dynamics simulations using one protein structure in the presence of the ligand of the other protein structure (referred to as the *cross-liganded* form) to investigate the dynamics of the peptide bond between Asp11 and Thr12. The two cross-liganded forms were thus prepared by simply superimposing all heavy atoms of one structure onto the other and replacing the ligand as appropriate.

Molecular dynamics simulations

Energy minimisations

Full energy minimisations were conducted on each crystal structure (PDB codes 1LAH and 1LST) using the Discover3 module of Insight2000 (Accelrys, Inc.) with the CFF forcefield [47]. Hydrogen atoms were previously added using the Biopolymer module assuming a pH of 7.4 to retain all available electrostatic interactions of ionisable sidechains with the ligands [35, 37]. A dielectric constant of 1.0 was used throughout. The minimisations were conducted in stages. Initially an energy minimisation was conducted only on the hydrogen atoms whilst the rest of the protein was kept rigid. During the second stage the sidechains of the protein were allowed to relax whilst the backbone was kept fixed. During the final stage the whole protein was allowed to relax. The energy minimisation procedure was carried out in the presence of the corresponding bound ligand, which was kept fixed at all times. The first and second stages of the minimisation involved 250 iterations of steepest descents (SD) followed by 500 iterations of conjugate gradients (CG). The final stage, where the whole protein was minimised, involved 250 iterations of SD followed by a maximum of 50,000 iterations of CG. The minimisation was terminated when the gradient of the energy converged to a value of less than 0.001 kcal/mol/Å.

Simulation conditions

Molecular dynamics (MD) simulations were performed using the Discover3 module of Insight2000 (Accelrys, Inc.) with the CFF forcefield [47]. The energy-minimised protein structures were used as the input for these simulations. The unliganded, ornithine-bound and lysine-bound forms are referred to hereafter as the 'free', 'orn' and 'lys' forms, respectively.

The equilibrium properties of these systems were sampled in the NVT ensemble. Each simulation was run for 1010,000 steps with a short 0.5 fs time step (to ensure energy conservation given the high temperature used in the simulations) for a total simulation time of 505 ps, of which the last 500 ps were used for analysis. In each trajectory, the atomic coordinates were saved by taking a snapshot of the simulation every 50 fs during the last 500 ps, for a total of 10,000 frames. As described below, some simulations were run for 2.05 ns.

All simulations were performed at a constant temperature of 500 K in order to accelerate conformational sampling, except for two initial simulations carried out at 300 K for comparison. The Nose-Hoover thermostat [48, 49] was used with a temperature window of 10 K. The equations of motion were integrated using the Verlet algorithm [50]. All covalent bonds between hydrogens and heavy atoms were constrained using the SHAKE algorithm [51]. The simulations were performed in vacuo as the binding site is known to be shielded from the solvent [35, 37] and hence there is no advantage in solvating the protein. In total, fourteen simulations were performed under various conditions, as listed in Table 2.

The simulations were performed at three levels of complexity. At the simplest level, the simulations allowed flexibility only for the segment where the backbone conformational change is observed (the peptide bond between Asp11 and Thr12). For this purpose, a segment contiguous to these residues was defined to allow enough conformational flexibility for the backbone conformational change of interest to take place. Two more residues on each side of Asp11 and Thr12 were considered, resulting in a flexible segment encompassing the segment Gly9-Thr10-Asp11-Thr12-Thr13-Tyr14. The rest of the protein was kept rigid. At the next level, the simulations allowed flexibility of the extended binding site (as defined above) in order to assess the influence that neighbouring regions to the above

Table 2 Summary of simulation conditions

System	PDB code	Ligand	Temperature (K)	Flexible region
1lst-free1	1LST	–	300	9–14
1lst-free2	1LST	–	500	9–14
1lst-free3	1LST	–	500	Binding site
1lst-free4*	1LST	–	500	Binding site
1lst-orn1	1LST	Orn	500	9–14
1lst-orn2	1LST	Orn	500	9–14 + Orn
1lst-orn3	1LST	Orn	500	Binding site + Orn
1lah-free1	1LAH	–	300	9–14
1lah-free2	1LAH	–	500	9–14
1lah-free3	1LAH	–	500	Binding site
1lah-free4[a]	1LAH	–	500	Binding site
1lah-lys1	1LAH	Lys	500	9–14
1lah-lys2	1LAH	Lys	500	9–14 + Lys
1lah-lys3	1LAH	Lys	500	Binding site + Lys

[a] These simulations were performed for 2.005 ns with the last 2.0 ns used for data collection

flexible segment within the binding site may have on the conformational changes in Asp11 and Thr12. The rest of the protein was kept rigid. Finally, simulations allowing flexibility of both the 9–14 segment and the extended binding site were carried out for the cross-liganded forms of the proteins. This was done to determine how the bound ligand may affect or indeed induce the conformational change. As before, the rest of the protein was kept rigid. These simulations were done with two variations: one allowing flexibility of both the protein (9–14 segment and binding site only) and the ligand, and another allowing flexibility of the protein (9–14 segment and binding site only) but keeping the ligand rigid and fixed in its bound conformation.

Analysis of simulation trajectories

The analysis of the MD trajectories was simplified by the fact that the simulations were performed only on the binding site of each protein whilst the rest of the protein was kept fixed. This eliminated the possibility of observing interdomain conformational changes that might have occurred because of the intrinsic flexibility of the linker region of the protein when simulating the unliganded form (as indeed has been observed in other reported molecular dynamics simulations [44]), which would have resulted in the opening up of the binding site of the protein.

Measurement of the Φ/ψ angles

Table 3 reports the Φ/ψ angles around the Asp11-Thr12 peptide bond after energy minimisation. Whilst the Φ/ψ angles predictably changed after energy minimisation, the two conformations remained very distinct. The two conformations were compared by measuring the angle between the planes containing the Asp11-Thr12 peptide bonds. This angle was measured initially to be 122° in the crystal structure [37], changing to 95° upon energy minimisation in the presence of the ligand, and to 94° upon energy minimisation without the ligand. For consistency, the Φ/ψ angles of Asp11 and Thr12 after energy minimisation in the presence of the corresponding ligand (see column 4 in Table 3) was used as the reference conformation for further comparisons.

Energy minimisation of the simulation trajectory snapshots

As described above, every single snapshot in each simulation trajectory was energy minimised before the Φ/ψ angles were measured. The energy minimisations were carried out using the same conditions as stated before. During the minimisations, all the atoms that were allowed flexibility during the MD simulations were optimised, whilst the rest of the protein was kept fixed. Each structure was subjected to 500 iterations of steepest descents (SD) followed by a maximum of 10,000 iterations of conjugate gradients (CG). The minimisations were terminated when the gradient of the energy converged to a value of less than 0.001 kcal/mol/Å.

Since the MD simulations were performed allowing flexibility only in either the 9–14 segment or the whole binding site, whilst keeping the rest of the protein fixed, the overall stability of the protein structure was maintained. However, in order to analyse the results, the fluctuations of the peptide bonds of every residue involved in the simulations (residues 9–14, or those making up the whole active site) were recorded. This was achieved by measuring both the Φ/ψ angles and the RMSDs (with respect to the reference residues) of every flexible residue that was involved in the simulation in each snapshot of the trajectory before and after energy minimisation.

Results and discussion

Simulations at 300 K

Two initial MD simulations were performed at 300 K on the free (unliganded) forms of PDB structures 1LST and 1LAH, allowing conformational flexibility only on segment 9–14 of the protein (simulations 1lst-free1 and 1lah-free1, as

Table 3 Φ/ψ angles of Asp11 and Thr12 of the LAOBP before and after energy minimisation

PBD code	Residue/Angle	Crystal structure[40]	Minimisation with ligand	Minimisation without ligand
1LST	Asp 11 Φ	−94.5	−74.7	−75.1
	Asp 11 ψ	112.7	160.6	156.9
	Thr 12 Φ	−85.0	−131.6	−131.1
	Thr 12 ψ	32.2	42.7	33.6
1LAH	Asp 11 Φ	−88.3	−87.9	−85.9
	Asp 11 ψ	−15.1	−52.5	−50.9
	Thr 12 Φ	58.3	81.6	80.7
	Thr 12 ψ	9.8	33.1	33.5
Angle between peptide bonds		122	95	94

outlined in Table 2). The Φ/ψ angles of Asp11 and Thr12 were monitored from the simulation snapshots before and after energy minimisation. Figures 2 and 3 show plots of these angles for the simulations of the 1LST and 1LAH structures, respectively.

Figure 2a shows that the Φ angle of Asp11 varied from −55.22° to −108.94°, whilst the corresponding ψ angle varied from 128.60° to −158.62° (in these plots an angle of 180° is the same as an angle of −180°). In the case of Thr12, Fig. 2c shows that the Φ angle varied from −154.75° to −104.76°, whilst the ψ angle varied from −8.24° to −76.04°. During the simulation the Φ/ψ angles of both Asp11 and Thr12 were always closer to the reference conformation of 1LST (shown in red dots) than to the alternative conformation seen in 1LAH (shown in green dots). In order to simplify the comparison of the conformations, Fig. 2b and d show plots of the corresponding Φ/ψ angles of Asp11 and Thr12, respectively, after energy minimisation of the snapshots. Upon energy minimisation the Φ angle of Asp11 ranged from −71.65° to −87.86° and the ψ angle ranged from 160.36° to 176.83°. Both angles match accurately the reference conformation of 1LST. The Φ angle of Thr12 ranged from −137.38° to −131.55° and the ψ angle ranged from 24.30° to 53.24°, in both cases matching closely the

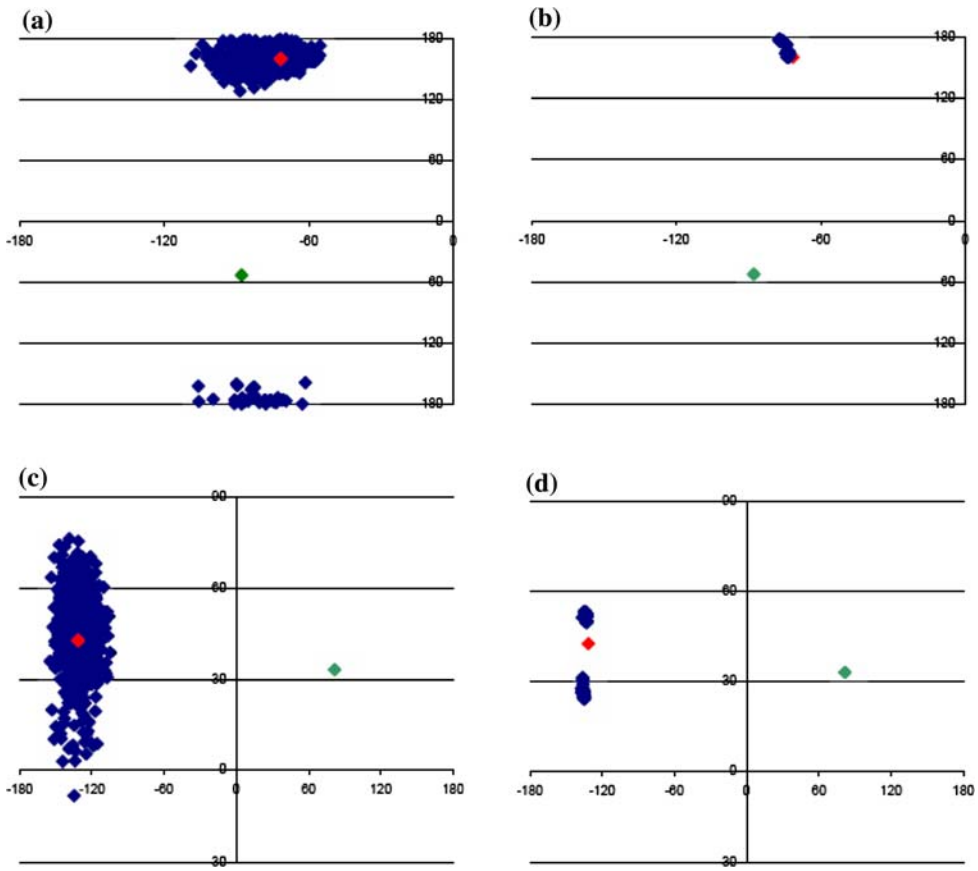

Fig. 2 Plots of the Φ/ψ angles of Asp11 and Thr12 for the 1lst-free1 simulation. The Φ angle was plotted on the *X*-axis and the ψ angle was plotted on the *Y*-axis. The reference Φ/ψ angles of 1LST and 1LAH are shown in red and green, respectively. The Φ/ψ angles of each snapshot are shown in blue: (**a**) The Φ/ψ angle plot of Asp11 before minimisation; (**b**) The Φ/ψ angle plot of Asp11 after minimisation; (**c**) The Φ/ψ angle plot of Thr12 before minimisation; (**d**) The Φ/ψ angle plot of Thr12 after minimisation

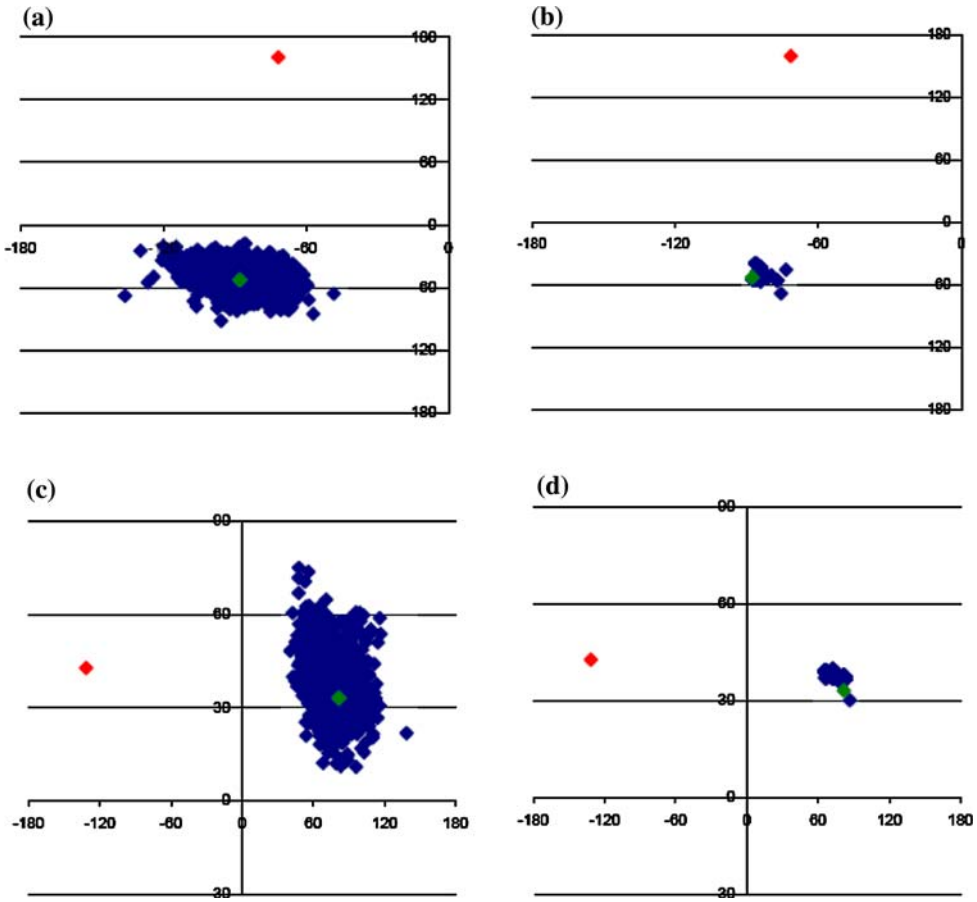

Fig. 3 Plots of the Φ/ψ angles of Asp11 and Thr12 for the 1lah-free1 simulation. The Φ angle was plotted on the *X*-axis and the ψ angle was plotted on the *Y*-axis. The reference Φ/ψ angles of 1LST and 1LAH are shown in red and green, respectively. The Φ/ψ angles of each snapshot are shown in blue: (**a**) The Φ/ψ angle plot of Asp11 before minimisation; (**b**) The Φ/ψ angle plot of Asp11 after minimisation; (**c**) The Φ/ψ angle plot of Thr12 before minimisation; (**d**) The Φ/ψ angle plot of Thr12 after minimisation

reference conformation of 1LST. Visual inspection of some of these snapshots confirmed that the conformation of the peptide bond between Asp11 and Thr12 was the same as that in the reference structure 1LST.

Figure 3a shows that the Φ angle of Asp11 varied from −136.15° to −48.23°, whilst the corresponding ψ angle varied from −91.77° to −17.63°. In the case of Thr12, Fig. 3c shows that the Φ angle of Thr12 varied from 40.54° to 138.67°, whilst the ψ angle varied from 10.83° to −74.94°. During the simulation the Φ/ψ angles of both Asp11 and Thr12 were always closer to the reference conformation of 1LAH (shown in green dots) than to the alternative conformation seen in 1LST (shown in red dots). In order to simplify the comparison of the conformations, Fig. 3b and d show plots of the corresponding Φ/ψ angles of Asp11 and Thr12, respectively, after energy minimisation of the snapshots. Upon energy minimisation the Φ angle of Asp11 ranged from −87.50° to −78.60° and the ψ angle of Asp11 ranged from −67.93° to −39.63°. Both angles match accurately the reference conformation of 1LAH. The Φ angle of Thr12 ranged from 65.77° to 86.94° and the ψ angle of Thr12 ranged from 30.14° to 39.75°, in both cases matching closely the reference conformation of 1LAH. Visual inspection of some of these snapshots confirmed that the conformation of the peptide bond between Asp11 and Thr12 was the same as that in the reference structure 1LAH.

Both simulations described above produced analogous results. Whilst the Φ/ψ angles of Asp11 and Thr12 fluctuated several tens of degrees during the simulations, no interconversion between conformations A (seen in structure 1LST) and B (seen in structure 1LAH) was observed in either of the simulations. The backbone conformations visited by these fluctuations were largely reduced and clustered upon energy minimisation to a small number of local conformational energy minima, which generally matched the initial minimised conformations of the reference structures.

The time evolution of the Φ/ψ angles for all the amino acids in the 9–14 segment was also monitored. It was observed that the Φ/ψ angles of residues Gly9, Thr10, Thr13 and Tyr14 fluctuated to a much smaller degree than the above reported Φ/ψ angles of Asp11 and Thr12 (results not shown). This reveals that most of the backbone movement of the 9–14 segment is due to fluctuations in the Φ/ψ angles of Asp11 and Thr12 only.

Simulations at 500 K

The previous simulations showed that the conformation of the backbone of the 9–14 segment remains largely

unchanged (except for Asp11 and Thr12) during the simulations at 300 K. Consequently all remaining simulations were carried out at 500 K in order to accelerate conformational sampling in all the various simulation conditions (see Table 2).

Simulations of the 9–14 segment

The next set of MD simulations was carried out also on the free (unliganded) forms of PDB structures 1LST and 1LAH, once again allowing conformational flexibility only on segment 9–14 of the protein (simulations 1lst-free2 and 1lah-free2, as outlined in Table 2). As before, the Φ/ψ angles of Asp11 and Thr12 were monitored from the simulation snapshots before and after energy minimisation, although we focus here only on the latter. Figure 4 shows plots of these minimised angles for the simulations of the 1LST and 1LAH structures, in a similar fashion to Figs. 2b, d and 3b, d.

The key difference in these high temperature simulations is that in the simulation of the free 1LST structure (1lst_free2), the Φ/ψ angles of Asp11 and Thr12 shifted from those of the reference 1LST structure (conformation A) to those of the 1LAH structure (conformation B). This suggests that a higher temperature was indeed required for the simulations to adequately sample conformational space in order for rotation of the Asp11-Thr12 peptide bond to take place. On the other hand, the Φ/ψ angles of Asp11 and Thr12 of the unliganded 1LAH structure (1lah_free2) remained the same throughout the simulation and no conformational change was observed.

As before, the time evolution of the Φ/ψ angles for all the amino acids in the 9–14 segment was monitored. Despite the higher temperature, it was observed again that the Φ/ψ angles of residues Gly9, Thr10, Thr13 and Tyr14 fluctuated to a much smaller degree than the Φ/ψ angles of Asp11 and Thr12 (results not shown). This provided further evidence that any backbone movement of the 9–14 segment is likely to arise due to fluctuations in the Φ/ψ angles of Asp11 and Thr12 only.

The backbone conformation of Asp11 and Thr12 (conformation A), as seen in the 1LST structure is also observed in all other X-ray structures (with the exception of the 1LAH structure, exhibiting conformation B), suggesting that conformation A may be the most stable conformation. However, these simulations seem to suggest that the preferred backbone conformation of Asp11 and Thr12 might indeed be conformation B, which both simulations at 500 K converged to regardless of the initial conformation. There are several possible explanations for this observation:

(1) Conformation B of Asp11 and Thr12 is indeed the most stable one.
(2) Conformation B of Asp11 and Thr12 in the 1LAH structure is more favoured *only* in the 'closed unliganded' form. As the 1LST and 1LAH structures were simulated without the presence of the ligand, the structures can be regarded as 'closed unliganded' forms. However, the unliganded LAOBP has an open conformation whilst the closed conformation is only observed experimentally in its ligand-bound form [37].
(3) This observation is due to insufficient conformational sampling, and longer simulations would have revealed that both conformations are visited regardless of the initial conformation of the backbone of Asp11 and Thr12.

Simulations of the cross-liganded forms

In order to find more evidence in relation to the above hypotheses, new simulations were performed on the 'cross-liganded' forms. These simulations were expected to give an indication as to whether the conformational changes that seem to favour conformation B (from the 1LAH structure) are influenced by the ligand present.

The next set of MD simulations was carried out on the cross-liganded forms of PDB structures 1LST and 1LAH, once again allowing conformational flexibility only on segment 9–14 of the protein and keeping the ligand rigid and fixed in its original position (simulations 1lst-orn1 and 1lah-lys1, as outlined in Table 2). As before, the Φ/ψ angles of Asp11 and Thr12 were monitored from the simulation snapshots before and after energy minimisation. Figure 5 shows plots of these minimised angles for the simulations of the 1LST and 1LAH structures, as before.

Figures 5a and b reveal that the minimised Φ/ψ angles of Asp11 and Thr12 fluctuate in the vicinity of the minimised reference 1LST conformation and that there is no conformational change. At the same time, Fig. 5c and d reveal that the distribution of minimised Φ/ψ angles of both Asp11 and Thr12 remained in the vicinity of the reference minimised conformation, with a similar distribution to that seen in the previous simulations of the free (unliganded) 1LAH structure (simulations 1lah-free1 and 1lah-free2).

There is the distinct possibility that the previously observed conformational change of Asp11 and Thr12 (conformation A–B) in the absence of bound ligand (the 1lst_free2 simulation) was now not observed in the presence of the cross-ligand because the ligand was kept rigid and fixed during the simulation. Consequently, a further set of simulations was performed under the same conditions but this time allowing full conformational flexibility and translational freedom in the ligand (simulations 1lst-orn2 and 1lah-lys2, as outlined in Table 2). Figure 6 shows plots of the minimised Φ/ψ angles of Asp11 and Thr12 angles.

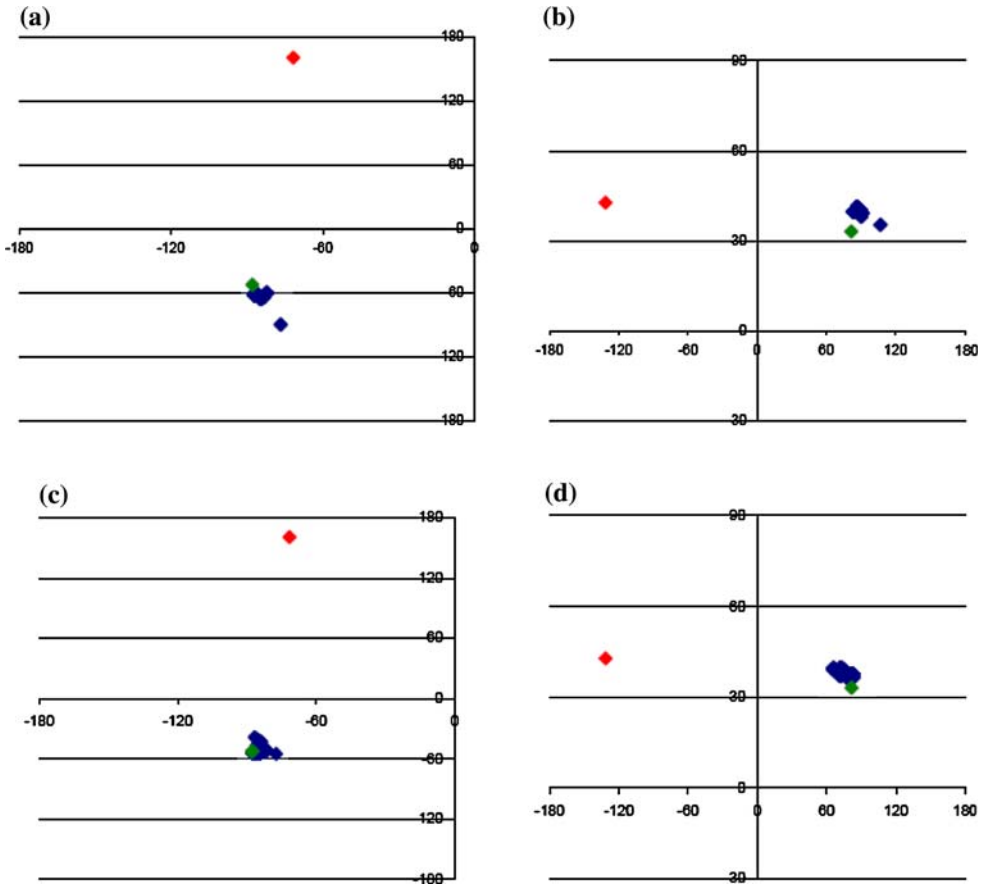

Fig. 4 Plots of the Φ/ψ angles of Asp11 and Thr12 for the 1lst-free2 and 1lah-free2 simulations after energy minimisation. The Φ angle was plotted on the *X*-axis and the ψ angle was plotted on the *Y*-axis. The reference Φ/ψ angles of 1LST and 1LAH are shown in red and green, respectively. The Φ/ψ angles of each snapshot are shown in blue: (**a**) The Φ/ψ angle plot of Asp11 of 1lst-free2; (**b**) The Φ/ψ angle plot of Thr12 of 1lst-free2; (**c**) The Φ/ψ angle plot of Asp11 of 1lah-free2; (**d**) The Φ/ψ angle plot of Thr12 of 1lah-free2

Figure 6a and b reveal that the minimised Φ/ψ angles of Asp11 and Thr12 match those in the 1LAH structure, showing that a change to conformation B has occurred again. The plots also reveal that the minimised Φ/ψ angles of Asp11 and Thr12 also fluctuate in the vicinity of conformation A (this was confirmed upon visual inspection of selected snapshots), suggesting that both conformations were visited during the simulation. At the same time, Fig. 6c and d reveal that the distribution of minimised Φ/ψ angles of both Asp11 and Thr12 remained in the vicinity of the reference minimised conformation (structure 1LAH). Consequently all the simulations performed so far on the 1LAH structure (1lah_free2, 1lah_lys1 and 1lah_lys2) indicate that the backbone conformation of Asp11 and Thr12 (conformation B) remains the same with or without the bound cross-ligand.

Simulations at 500 K of the 1LST structure reveal that Asp11 and Thr12 switch from conformation A to B, and that this conformational change can occur both in the free and cross-liganded forms. However, translational and internal flexibility of the ligand is essential for the A→B conformational change to take place. This suggests a ligand-induced conformational change, whereby the dynamic binding of ornithine would stabilise the conformation of Asp11 and Thr12 as seen in the 1LAH structure (conformation B).

The RMSD of ornithine with respect to its initial conformation and its position with respect to the 1LST structure (the cross-liganded form) were monitored during the simulation (results not shown). The RMSD (of all heavy atoms) of ornithine with respect to its initial conformation ranged between 0.05 Å and 2.59 Å, with an average RMSD of 0.89 Å. The distance between the centre of mass of ornithine and its absolute initial position ranged between 0.1 and 0.6 Å. This indicates that ornithine remained close to its original binding location during the simulation but exhibited a certain degree of conformational flexibility.

It seems that the presence of ornithine in the 1LST cross-liganded structure restricts the movement of the sidechain of Asp11, but only when the ligand is kept rigid during the simulation (1lst-orn1). As a consequence, the concomitant rotation of the Asp11-Thr12 peptide bond is impeded. A more realistic simulation allowing ornithine to have conformational and translational freedom (1lst-orn2) allows the concerted movement of the sidechain of Asp11 and the rotation of the Asp11-Thr12 peptide bond, resulting

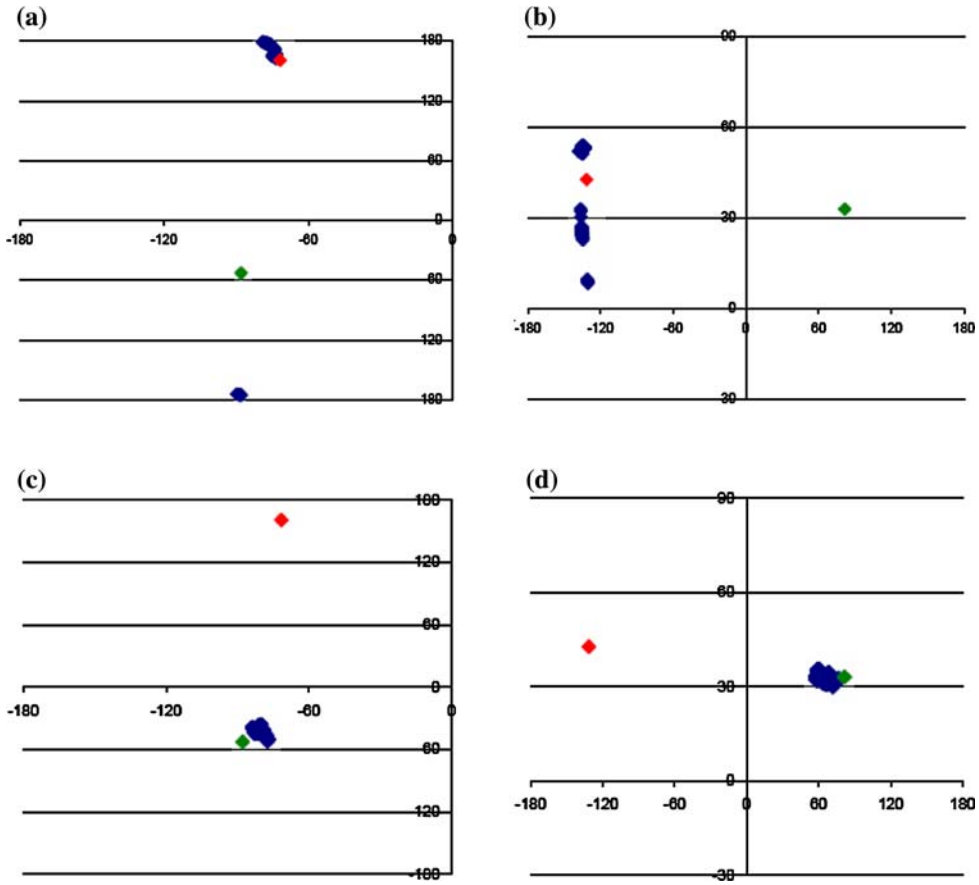

Fig. 5 Plots of the Φ/ψ angles of Asp11 and Thr12 for the 1lst-orn1 and 1lah-lys1 simulations after energy minimisation. The Φ angle was plotted on the *X*-axis and the ψ angle was plotted on the *Y*-axis. The reference Φ/ψ angles of 1LST and 1LAH are shown in red and green, respectively. The Φ/ψ angles of each snapshot are shown in blue: (**a**) The Φ/ψ angle plot of Asp11 of 1lst-orn1; (**b**) The Φ/ψ angle plot of Thr12 of 1lst-orn1; (**c**) The Φ/ψ angle plot of Asp11 of 1lah-lys1; (**d**) The Φ/ψ angle plot of Thr12 of 1lah-lys1

in the observed change of the backbone of Asp11 and Thr12 from conformation A to B.

Simulations of the binding site

The above simulations kept most of the binding site rigid, allowing flexibility only on the 9–14 segment. This approach was consistent with the fact that the interdomain conformational change of the LAOBP follows essentially a rigid body motion with very little conformational change in the binding site [35, 37, 40, 42, 44]. Whilst the simulations of the 9–14 segment showed very little motion beyond Asp11 and Thr 12, further simulations were performed allowing full flexibility of the binding site to investigate whether there is any influence of the dynamics of the binding site on the conformational changes that seem to favour conformation B.

A first set of simulations was performed on the free (unliganded) forms (1lst-free3 and 1lah-free3), allowing full flexibility of the whole binding site. The simulations were otherwise conducted in the same conditions as described above. The Φ/ψ angles of Asp11 and Thr12 were monitored from the simulation snapshots before and after energy minimisation. Figure 7 shows plots of these minimised angles for the simulations of the 1LST and 1LAH structures, as before.

Figure 7a and b reveal that the minimised Φ/ψ angles of Asp11 and Thr12 fluctuate in the vicinity of the minimised reference 1LST conformation and that there is no conformational change. The plots also suggest that the minimised Φ/ψ angles of Asp11 and Thr12 also fluctuated around other conformations, but these were not close enough to conformation B (this was confirmed by visual inspection of selected snapshots). At the same time, Fig. 7c and d reveal that the distribution of minimised Φ/ψ angles of both Asp11 and Thr12 remained in the vicinity of the reference minimised conformation (structure 1LAH).

No conformational change around Asp11 and Thr12 was observed, although it seems that it was close to occurring with structure 1LST. Since the system involves a larger number of flexible amino acids, these simulations were repeated and the simulation time was extended to 2.05 ns, in order to ensure sufficient conformational sampling (1lah-free4 and 1lst-free4). Figure 8 shows plots of these minimised angles for the simulations of the 1LST and 1LAH structures, as before.

Figure 8a and b reveal that the minimised Φ/ψ angles of Asp11 and Thr12 match those in the 1LAH and the 1LST structure, showing that a change to conformation B occurred again but that both conformations were visited during the simulation. An examination of the Φ/ψ angles

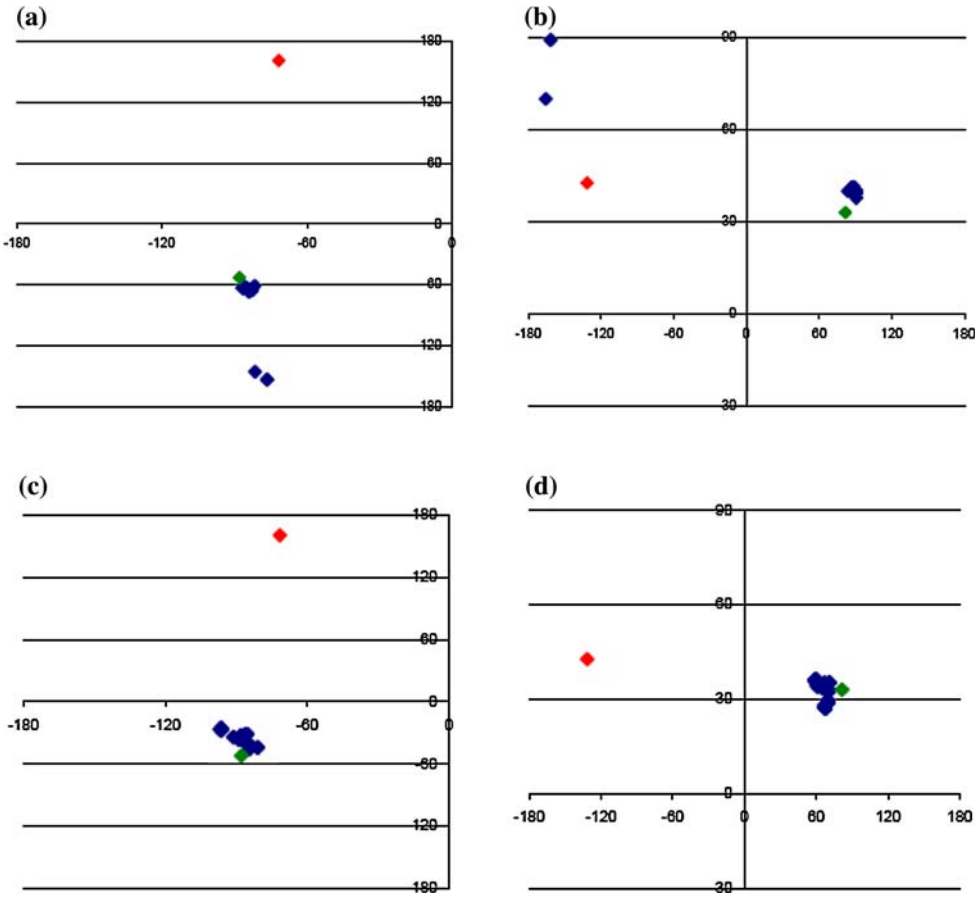

Fig. 6 Plots of the Φ/ψ angles of Asp11 and Thr12 in the 1lst-orn2 and 1lah-lys2 simulations after energy minimisation. The Φ angle was plotted on the *X*-axis and the ψ angle was plotted on the *Y*-axis. The reference Φ/ψ angles of 1LST and 1LAH are shown in red and green, respectively. The Φ/ψ angles of each snapshot are shown in blue: (**a**) The Φ/ψ angle plot of Asp11 of 1lst-orn2; (**b**) The Φ/ψ angle plot of Thr12 of 1lst-orn2; (**c**) The Φ/ψ angle plot of Asp11 of 1lah-lys2; (**d**) The Φ/ψ angle plot of Thr12 of 1lah-lys2

along the simulation trajectory (results not shown) revealed that the first A→B conformational change occurred after 1.2 ns. Conformation B remained stable for about 550 ps, at which point a reverse B→A conformational change took place. Consequently, this longer simulation showed that the A→B conformational change is reversible. Interestingly, the average time scale of these local backbone conformational changes is similar to the reported time scale of conformational transitions between the closed and open forms of the LAOBP (less than 1.0 ns) [44].

Figure 8c and d reveal that the distribution of minimised Φ/ψ angles of both Asp11 and Thr12 remained in the vicinity of the reference minimised conformation, consistent with all previous simulations ran starting from the 1LAH structure.

A final set of simulations of the whole binding site was carried out on both cross-liganded forms (1lst-orn3 and 1lah-lys3). The simulations were conducted in the same conditions as described above. The ligands were allowed full conformational flexibility and translational freedom. The Φ/ψ angles of Asp11 and Thr12 were monitored from the simulation snapshots before and after energy minimisation. Figure 9 shows plots of these minimised angles for the simulations of the 1LST and 1LAH structures, as before.

The results are similar to those observed for the simulations of the 9–14 segment in the presence of the cross-ligands (simulations 1lst_orn2 and 1lah_lys2). Figure 9a and b reveal that the minimised Φ/ψ angles of Asp11 and Thr12 match those in the 1LAH structure, showing that a change from conformation A to B has taken place. On the other hand, Fig. 9c and d reveal that the distribution of minimised Φ/ψ angles of both Asp11 and Thr12 remained in the vicinity of the reference minimised conformation (structure 1LAH).

A summary of the results of all the simulations can be found in Table 4. In this table the central column indicates what portion of the LAOBP was allowed flexibility during the simulations, whilst columns 1 and 3 on either side indicate what conformations were observed during the simulations of each crystal structure. In the case of the simulations using the 1LAH structure, in all cases the backbone conformation of Asp11 and Thr12 remained the same (conformation B) throughout the simulations. We did not observe a B→A conformational change, regardless of the flexible region considered or the protein form simulated.

Different results were obtained in the case of the simulations using the 1LST structure. Simulations of the free (unliganded) form exhibited an A→B conformational change when either the whole binding site (long simulation)

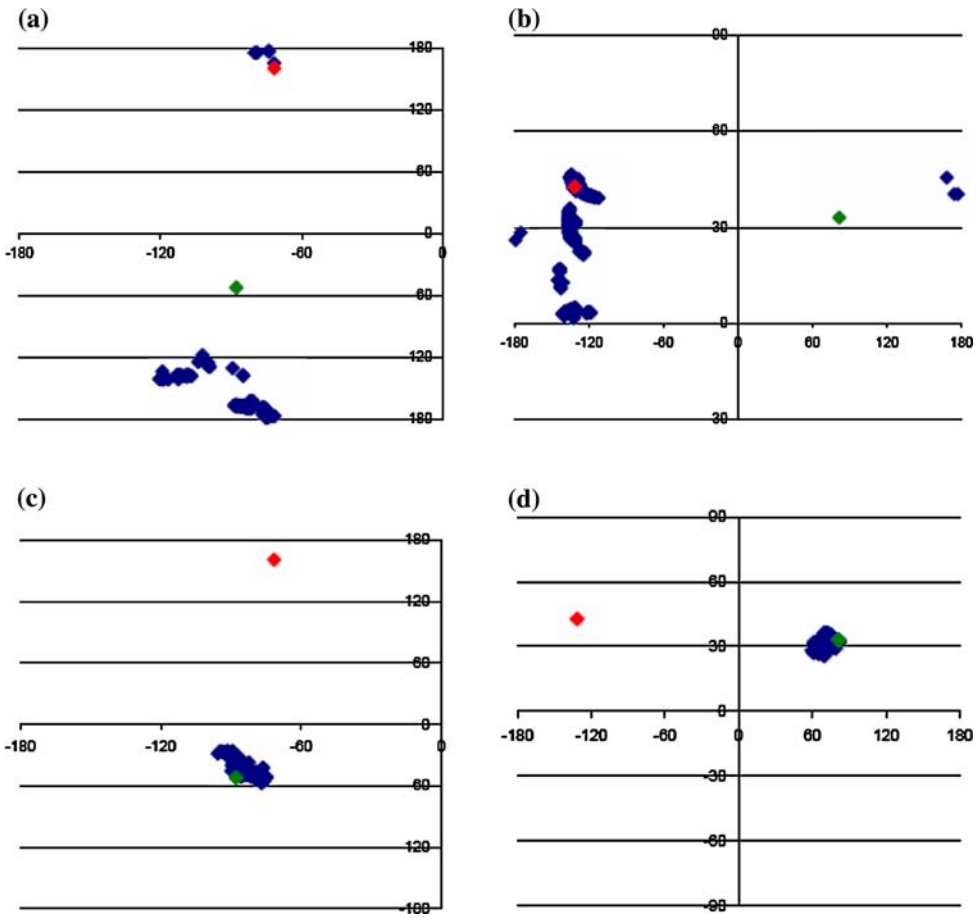

Fig. 7 Plots of the Φ/ψ angles of Asp11 and Thr12 in the 1lst-free3 and 1lah-free3 simulations after energy minimisation. The Φ angle was plotted on the *X*-axis and the ψ angle was plotted on the *Y*-axis. The reference Φ/ψ angles of 1LST and 1LAH are shown in red and green, respectively. The Φ/ψ angles of each snapshot are shown in blue: (**a**) The Φ/ψ angle plot of Asp11 of 1lst-free3; (**b**) The Φ/ψ angle plot of Thr12 of 1lst-free3; (**c**) The Φ/ψ angle plot of Asp11 of 1lah-free3; (**d**) The Φ/ψ angle plot of Thr12 of 1lah-free3

or just the 9–14 loop region was allowed flexibility. In addition, the long simulation of the binding site showed reversible A↔B conformational changes. When these simulations were done on the cross-liganded forms, the A→B conformational change was also observed, but only if the cross-ligand (ornithine) was allowed conformational flexibility and translational freedom. As discussed earlier, this is due to the fact that, if the cross-ligand remains fixed in its original position, there is a steric impediment that disallows the change in conformation of the sidechain of Asp11, thus preventing the concomitant rotation of the Asp11-Thr12 peptide bone.

Whilst both conformations A and B of the peptide bond between Asp11 and Thr12 are energetically favoured [37], our simulations reveal that both conformations are accessible from the 1LST structure (conformation A), but not from the 1LAH structure (conformation B). Hence ornithine is able to induce a conformational change in the backbone of Asp11 and Thr12, but lysine does not seem to be able to reverse it.

Energy analysis of conformations A and B

An energy analysis of the two protein structures (1LST and 1LAH) and their 9–12 segments was carried out to investigate the relative stability of conformations A and B. For this purpose, the whole structures of the ligand-protein complexes were fully minimised. Table 5 reports the energies of the proteins with and without the bound ligand. The energy of the unliganded form (protein only) of 1LST is lower than in 1LAH by 74.2 kcal/mol. However, in the ligand-bound (complex) forms, the 1LAH structure has only a slightly lower energy (by 2.55 kcal/mol) than the 1LST structure after a much larger reduction in energy upon ligand binding. This suggests that the stabilisation of the LAOBP structure is significantly higher with bound ornithine than with bound lysine. The differences in energy between the two protein structures are expected to arise not only from differences in the 9–14 segment, but also from small but cumulative differences between the two crystal structures, such as different rotamers on sidechains on the surface of the proteins and small variations in dihedral angles across the whole structure. Whilst the two structures clearly possess the same overall architecture (closed conformation), such small differences in structure give rise to differences in the computed potential energy. It is not uncommon for very similar structures to have different energies, as well as for structures with very similar energies to have different structures. Consequently we have focused

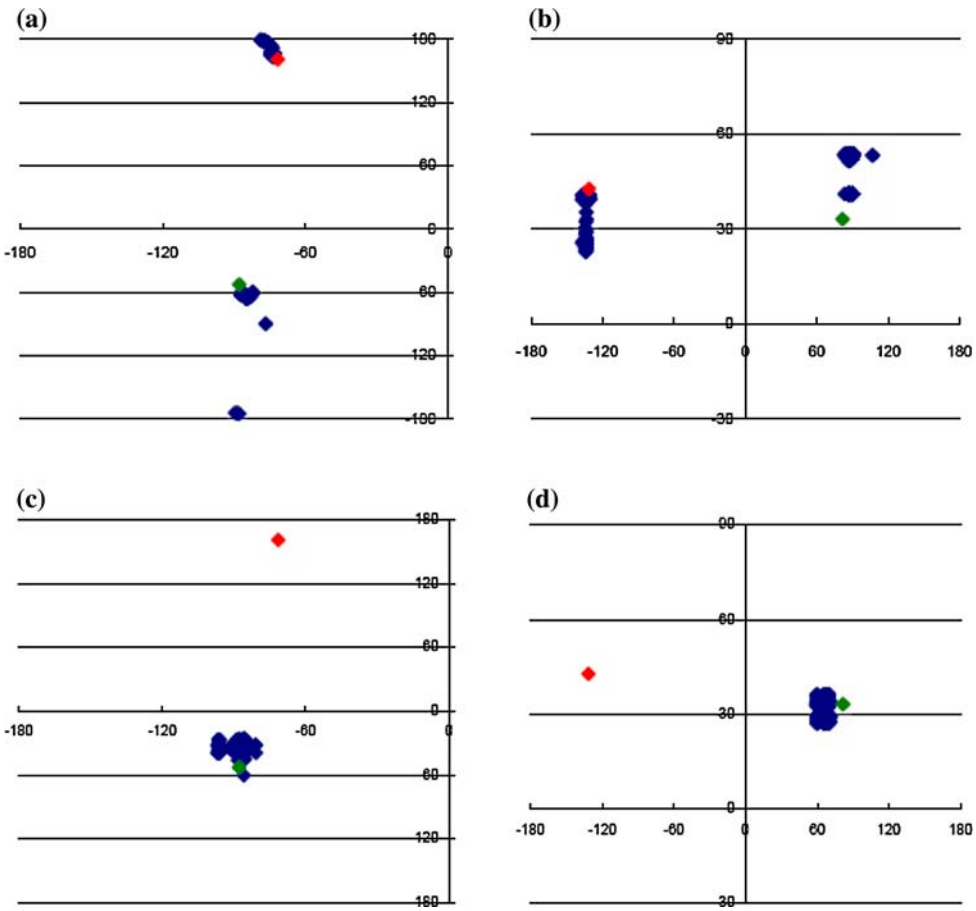

Fig. 8 Plots of the Φ/ψ angles of Asp11 and Thr12 in the 1lst-free4 and 1lah-free4 simulations. The Φ angle was plotted on the *X*-axis and ψ angle was plotted on the *Y*-axis. The reference Φ/ψ angles of 1LST and 1LAH are shown in red and green, respectively. The Φ/ψ angles of each snapshot are shown in blue: (**a**) The Φ/ψ angle plot of Asp11 of 1lst-free4; (**b**) The Φ/ψ angle plot of Thr12 of 1lst-free4; (**c**) The Φ/ψ angle plot of Asp11 of 1lah-free4; (**d**) The Φ/ψ angle plot of Thr12 of 1lah-free4

on the energy difference between the unliganded and liganded forms of the same protein structure.

The larger energy reduction in the 1LAH complex structure may explain why ornithine was able to induce conformation B in the simulations of the 1LST structure, whilst lysine was not able to induce conformation A in the simulations of the 1LAH structure. The energies of the unliganded and liganded forms include contributions from the whole energy-minimised protein molecule. As stated above, since the overall structures of 1LST and 1LAH are similar but not identical, we decided to measure the energies of the 9–14 segments only to investigate their contribution to the energy of conformations A and B upon ligand binding.

The energy of the 9–14 segments (extracted from the minimised protein) and of their backbone atoms alone in both structures are also shown in Table 5. The energy of the 9–14 segment from the 1LAH structure is lower by 37.51 kcal/mol than that from the 1LST structure. This energy difference accounts for just over half of the difference in energy between the two protein structures (see above), confirming that the main structural changes affecting the potential energy of the proteins are dictated by the 9–14 segment. As stated in the Introduction, the main difference between conformations A and B reside in the backbone conformation between Asp11 and Thr 12, as well as the sidechain conformation of Asp11. The backbone (main chain atoms) alone accounts for 10.18 kcal/mol in the energy difference of the 9–14 segment. These energy differences suggest that the 9–14 segment in the 1LAH structure (conformation B) is more stable than in the 1LST structure (conformation A). Consequently, it should be easier for the A→B conformational change to take place than for the reverse.

Conclusions

Comprehensive molecular dynamics simulations have been performed for the two backbone conformations of Asp11 and Thr12 in the LAOBP. The simulations suggest that the backbone conformation of Asp11 and Thr12 of PDB structure 1LAH is the preferred conformation, as no other conformation was observed. On the other hand, simulations of the closed unliganded form of PDB structure 1LST revealed that the backbone conformations of Asp11 and Thr12 seen in the 1LAH and 1LST structures are observed when the 1LST structure is used. A simulation performed on

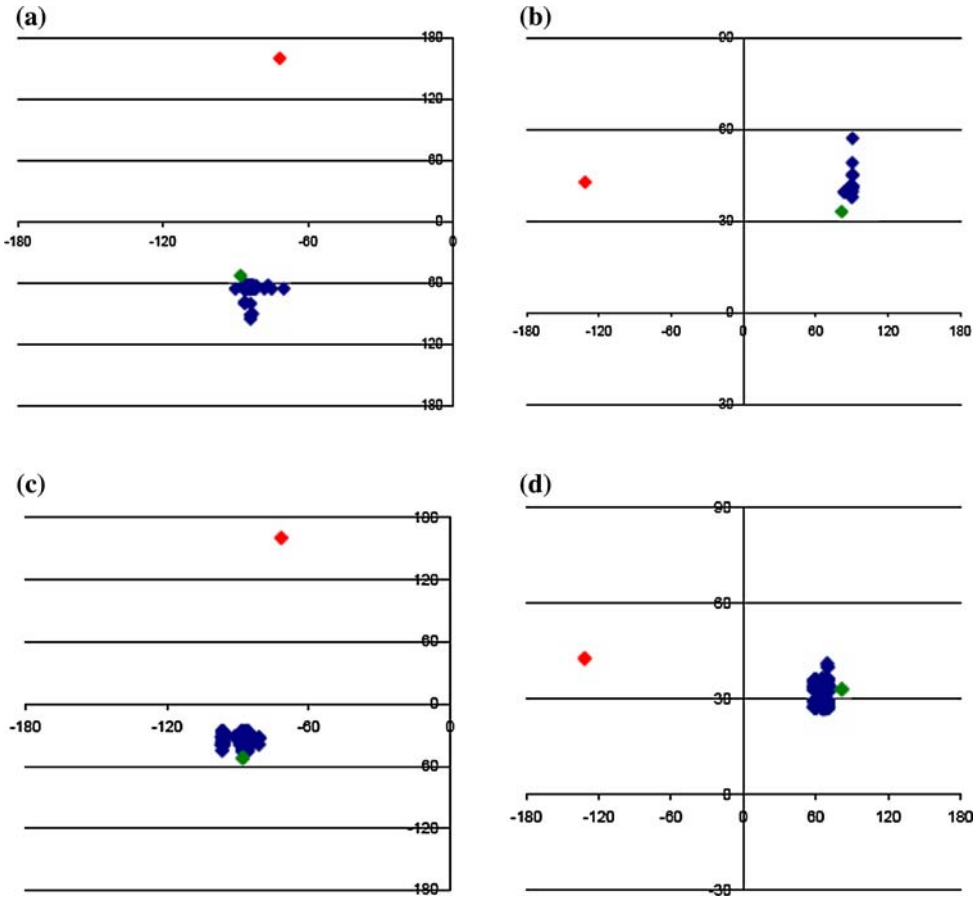

Fig. 9 Plots of the Φ/ψ angles of Asp11 and Thr12 in the 1lst-orn3 and 1lah-lys3 simulations. The Φ angle was plotted on the *X*-axis and the ψ angle was plotted on the *Y*-axis. The reference Φ/ψ angles of 1LST and 1LAH are shown in red and green, respectively. The Φ/ψ angles of each snapshot are shown in blue: (**a**) The Φ/ψ angle plot of Asp11 of 1lst-orn3; (**b**) The Φ/ψ angle plot of Thr12 of 1lst-orn3; (**c**) The Φ/ψ angle plot of Asp11 of 1lah-lys3; (**d**) The Φ/ψ angle plot of Thr12 of 1lah-lys3

Table 4 Summary of simulation results (at 500 K)

Conformation observed[a] (starting from 1LST)	Flexible portion of the protein	Conformation observed[a] (starting from 1LAH)
B	9–14 segment	B
A	9–14 segment (+Orn[b])	
	9–14 segment (+Lys[b])	B
A + B	9–14 segment + Orn	
	9–14 segment + Lys	B
A	Binding site	B
A + B	Binding site[c]	B
B	Binding site + Orn	
	Binding site + Lys	B

[a] Conformation A is that of the 1LST structure and conformation B is that of the 1LAH structure

[b] The ligand is present but kept rigid and fixed in its original crystallographic position

[c] Simulation time of 2.0 ns

Table 5 Conformational energies of the LAOBP

Structure	Energy (kcal/mol)			
	Protein only	Complex	9–14 segment[a]	9–14 backbone[b]
1LST	−6020.52	−6114.38	153.09	71.06
1LAH	−5946.32	−6116.93	115.58	60.88

[a] The 9–14 segment was extracted from the minimised structure. Missing hydrogens were added before measuring the energy

[b] The backbone of the 9–14 segment was defined by mutating the amino acids to glycine (hence replacing the sidechains with a hydrogen atom)

the cross-liganded form of the 1LST structure suggests that ornithine is able to induce a conformational change in Asp11 and Thr12, provided that the ligand is allowed full conformational flexibility and translational freedom. If ornithine is kept fixed then the sidechain of Asp11 experiences steric hindrance and cannot modify its conformation, which in turn prevents the rotation of the Asp11-Thr12 peptide bond. On the other hand, lysine bound to the 1LAH structure failed to induce the reverse conformational change.

An energy analysis revealed that the energy of the unliganded form of the 1LST structure is lower than that of the

1LAH structure. However, ornithine stabilises the complex and as a result the energy of the liganded form of the 1LAH structure becomes lower than that of the liganded form of the 1LST structure. Furthermore, the 9–14 segment has a lower energy in the 1LAH structure than in the 1LST structure. Consequently, when simulating the LAOBP in its 'closed unliganded' form, the backbone conformation of Asp11 and Thr12 found in the 1LAH structure is preferred over the conformation found in the 1LST structure.

Acknowledgements AYCY gratefully acknowledges De Novo Pharmaceuticals Ltd. for the award of a postgraduate scholarship. Part of this work was funded by a Strategic Research Grant from Curtin University of Technology.

References

1. Carlson HA, McCammon JA (2000) Accommodating protein flexibility in computational drug design. Mol Pharm 57:213–218
2. Carlson HA (2002) Protein flexibility is an important component of structure-based drug discovery. Curr Pharm Dis 8:1571–1578
3. Carlson HA (2002) Protein flexibility an drug design: how to hit a moving target. Curr Opin Chem Biol 6:447–452
4. Teague SJ (2003) Implications of protein flexibility for drug discovery. Nat Rev Drug Discov 2:527–541
5. Teodoro ML, Kavraki LE (2003) Conformational flexibility models for the receptor in structure based drug design. Curr Pharm Des 9:1635–1648
6. Wong CF, McCammon JA (2003) Protein flexibility and computer-aided drug design. Annu Rev Pharmacol Toxicol 43:31–35
7. Leach AR (1994) Ligand docking to proteins with discrete side chain flexibility. J Mol Biol 235:345–356
8. Totrov M, Abagyan R (1997) Flexible protein-ligand docking by global energy optimization in internal coordinates. Proteins Suppl 1:215–220
9. Nakajima N, Higo J, Kidera A, Nakamura H (1997) Flexible docking of a ligand peptide to a receptor protein by multicanonical molecular dynamics simulation. Chem Phys Lett 278:297–301
10. Schnecke V, Kuhn LA (2000) Virtual screening with solvation and ligand-induced complementarity. Perspect Drug Discov 20:171–190
11. Cavasotto CN, Abagyan RA (2004) Protein flexibility in ligand docking and virtual screening to protein kinases. J Mol Biol 337:209–225
12. Sherman W, Day T, Jacobson MP, Friesner RA, Farid R (2006) Novel procedure for modeling ligand/receptor induced fit effects. J Med Chem 49:534–553
13. Carlson HA, Masukawa K, McCammon JA (1999) Method for including the dynamic fluctuations of a protein in computer-aided drug design. J Phys Chem A 103:10213–10219
14. Pang Y-P, Kozikowski AP (1994) Prediction of the binding sites of huperizine A in acetylcholinesterase by docking studies. J Comput-Aided Mol Des 8:669–681
15. Knegtel RMA, Kuntz ID, Oshiro CM (1997) Molecular docking to ensembles of protein structures. J Mol Biol 266:424–440
16. Bouzida D, Rejto PA, Arthurs S, Colson AB, Freer ST, Gehlhaar DK, Larson V, Luty BA, Rose PW, Verkhivker GM (1999) Computer simulations of ligand-protein binding with ensembles of protein conformations: a Monte Carlo study of HIV-1 protease binding energy landscapes. Int J Quant Chem 72:73–84
17. Claussen H, Buning C, Rarey M, Lengauer T (2001) FlexE: efficient molecular docking considering protein structure variations. J Mol Biol 308:377–395
18. Osterberg F, Morris GM, Sanner MF, Olson AJ, Goodsell DS (2002) Automated docking to multiple target structures: incorporation of protein mobility and structural water heterogeneity in AutoDock. Proteins 46:34–40
19. Erickson JA, Jalaie M, Robertson DH, Lewis RA, Vieth M (2004) Lessons in molecular recognition: the effects of ligand and protein flexibility on molecular docking accuracy. J Med Chem 47:45–55
20. Källblad P, Todorov NP, Willems HMG, Alberts IL (2004) Receptor flexibility in the in silico screening of reagents in the S1' pocket of human collagenase. J Med Chem 47:2761–2767
21. Todorov NP, Buenemann CL, Alberts IL (2006) De novo ligand design to an ensemble of protein structures. Proteins 64:43–59
22. Jiang F, Kim SH (1991) "Soft docking": matching of molecular surface cubes. J Mol Biol 219:79–102
23. Gschwend DA, Good AC, Kuntz ID (1996) Molecular docking towards drug discovery. J Mol Rec 9:175–186
24. Ferrari AM, Wei BQ, Costantino L, Shoichet BK (2004) Soft docking and multiple receptor conformations in virtual screening. J Med Chem 47:5076–5084
25. Carlson HA, Masukawa KM, Rubins K, Bushman FD, Jorgensen WL, Lins RD, Briggs JM, McCammon JA (2000) Developing a dynamic pharmacophore model for HIV-1 integrase. J Med Chem 43:2100–2114
26. Meagher KL, Carlson HA (2004) Incorporating protein flexibility in structure-based drug discovery: using HIV-1 protease as a test case. J Am Chem Soc 126:13276–13281
27. Damm KL, Carlson HA (2007) Exploring experimental sources of multiple protein conformations in structure-based drug design. J Am Chem Soc 129:8225–8235
28. Wasserman ZR, Hodge CN (1996) Fitting an inhibitor into the active site of thermolysin: a molecular dynamics case study. Proteins 24:227–237
29. Di Nola A, Roccatano D, Berendsen HJC (1994) Molecular dynamics simulation of the docking of substrates to proteins. Proteins 19:174–182
30. Mangoni R, Roccatano D, Di Nola A (1999) Docking of flexible ligands to flexible receptors in solution by molecular dynamics simulation. Proteins 35:153–162
31. Najmanovich R, Kuttner J, Sobolev V, Edelman M (2000) Side-chain flexibility in proteins upon ligand binding. Proteins 39: 261–268
32. Yang AY-C, Källblad P, Mancera RL (2004) Molecular modelling prediction of ligand binding site flexibility. J Comput Aided Mol Des 18:235–250
33. Murray CW, Baxter CA, Frenkel AD (1999) The sensitivity of the results of molecular docking to induced fit effects: application to thrombin, thermolysin and neuraminidase. J Comput-Aided Mol Des 13:547–562
34. Kang C-H, Shin W-C, Yamagata Y, Bokcen S, Ames GF-L, Kim S-H (1991) Crystal structure of the lysine-, arginine-, ornithine-binding protein (LAO) from *Salmonella typhimurium* at 2.7 Å resolution. J Biol Chem 266:23893–23899
35. Oh B-H, Pandit J, Kang C-H, Nikaido K, Gokcen S, Ames GF-L, Kim S-H (1993) Three-dimensional structures of the periplasmic lysine/arginine/ornithine-binding protein with and without a ligand. J Biol Chem 268:11348–11355
36. Ames GF-L (1986) Bacterial periplasmic transport systems: structure, mechanism and evolution. Annu Rev Biochem 55: 397–425
37. Oh B-H, Ames GF-L, Kim S-H (1994) Structural basis for multiple ligand specificity of the periplasmic lysine-, arginine-, ornithine-binding protein. J Biol Chem 269:26323–26330

38. Quiocho FA, Ledvina PS (1996) Atomic structure and specificity of bacterial periplasmic receptors for active transport and chemotaxis: variation of common themes. Mol Microbiol 20:17–25
39. Nikaido K, Ames GF-L (1992) Purification and characterization of the periplasmic lysine-, arginine-, ornithine-binding protein (LAO) from *Salmonella typhimurium*. J Biol Chem 267:20706–20712
40. Flocco MM, Mowbray SL (1995) Cα-based torsion angles: a simple tool to analyze protein conformational changes. Protein Sci 4:2118–2122
41. Maiorov V, Abagyan R (1997) A new method for modeling large-scale rearrangements of protein domains. Proteins 27:410–424
42. Keskin O, Jernigan RL, Bahar I (2000) Proteins with similar architecture exhibit similar large-scale dynamic behaviour. Biophys J 78:2093–2106
43. Tama F, Sanejouand Y-H (2001) Conformational change of proteins arising from normal mode calculations. Protein Eng 14:1–6
44. Pang A, Arinaminpathy Y, Sansom MSP, Biggin PC (2005) Comparative molecular dynamics–similar folds and similar motions? Proteins 61:809–822
45. McLachlan AD (1982) Rapid comparison of protein structures. Acta Crystallogr A 38:871–873
46. Martin, A.C.R. http://www.bioinf.org.uk/software/profit/
47. Maple JR, Hwang M-J, Stockfisch TP, Dinur U, Waldman M, Ewig CS, Hagler AT (1994) Derivation of class II force fields 1. Methodology and quantum force field for the alkyl functional group and alkane molecules. J Comput Chem 15:162–182
48. Nosé S (1984) A unified formulation of the constant temperature molecular dynamics methods. J Chem Phys 81:511–519
49. Hoover WG (1985) Canonical dynamics: equilibrium phase-space distributions. Phys Rev A 31:1695–1697
50. Verlet L (1967) Computer "experiments" on classical fluids I. Thermodynamical properties of Lennard-Jones molecules. Phys Rev 159:98–103
51. Ryckaert JP, Ciccotti G, Berendsen HJC (1977) Numerical integration of the Cartesian equations of motion of a system with constraints: molecular dynamics of *n*-alkanes. J Comput Phys 23:327–341
52. Schaffer L, Verkhivker GM (1998) Predicting structural effects in HIV-1 protease mutants complexes with flexible ligand docking and protein side-chain optimization. Proteins 33:295–310
53. Frimurer TM, Peters GH, Iversen LF, Andersen HS, Moller NP, Olsen OH (2003) Ligand-induced conformational changes: improved predictions of ligand binding conformations and affinities. Biophys J 84:2273–2281
54. Taylor RD, Jewsbury PJ, Essex JW (2003) FDS: flexible ligand and receptor docking with a continuum solvent and soft core energy function. J Comput Chem 24:1637–1656